CRYSTAL STRUCTURE OF GILLESPITE, $BaFeSi_4O_{10}$

A. PABST,
University of California, Berkeley, California.

ABSTRACT

Gillespite has been studied by means of rotation, oscillation, Laue and powder *x*-ray patterns. It belongs to the space group D_{4h}^8—$P4/ncc$. The unit cell, $a = 7.495 \pm 0.010$ Å, $c = 16.050 \pm 0.010$ Å, contains 4 $BaFeSi_4O_{10}$.

A structure with eleven parameters has been found which yields satisfactory agreement of calculated and observed intensities. It is a silicate sheet structure with oxygen atoms in three kinds of positions and unshared corners of SiO_4 tetrahedra on both sides of the sheets. Single and double fourier summations give an excellent check on the structure. Interatomic distances are of expected magnitude. Barium has an 8-fold coordination and iron a 4-fold coordination.

The leaching of gillespite is discussed.

INTRODUCTION

Gillespite was described as a new mineral by Schaller[1] from a "small rock specimen collected from a moraine . . . near the head of Dry Delta, Alaska Range, Alaska." At first the crystal system to which it belongs was not established but it was found to be "optically uniaxial." Upon later reexamination[2] Schaller described it as tetragonal because it showed poor rectangular cleavage in addition to the eminent basal cleavage. Other minerals identified in the specimen from which gillespite was described were celsian, hedenbergite and quartz.

Gillespite has been found in only one other locality,[3] near Incline, Mariposa County, California. There it is found with the new mineral sanbornite, $BaSi_2O_5$, celsian, witherite (?), diopside, tourmaline, quartz and pyrrhotite. No geologic study of the occurrence has been made, but it is stated to be "probably from a contact metamorphic zone."

The *x*-ray data for this study were obtained during 1938–39 while the writer held a fellowship of the John Simon Guggenheim Memorial Foundation. Most of the diffraction patterns were made in the Department of Mineralogy of the British Museum of Natural History, the facilities of which were graciously made available by Dr. W. Campbell Smith and Mr. F. A. Bannister. One important pattern was also obtained in the crystallographic laboratory of the University of Cambridge through the courtesy of Dr. A. J. Bradley and Mr. H. Lipson. Later phases of

---

[1] Schaller, W. T., Gillespite, a new mineral: *Jour. Wash. Acad. Sci.*, **12,** 7–8 (1922).

[2] Schaller, W. T., The properties and associated minerals of gillespite: *Am. Mineral.* **14,** 319–322 (1929).

[3] Rogers, A. F., Sanbornite, a new barium silicate mineral from Mariposa County, California: *Am. Mineral.*, **17,** 161–172 (1932).

the work were aided by a grant from the Committee on Research of the University of California.

MATERIAL

Small fragments of nearly pure gillespite from the Alaska locality were kindly furnished by Dr. Schaller and Professor Rogers. Dr. A. A. Fitch gave some specimens of sanbornite from the California locality from which it was possible to separate a supply of clean fragments of gillespite. No difference whatever can be observed in the *x*-ray patterns of gillespite from the two localities.

CELL DIMENSIONS, CONTENT AND DENSITY

The cell dimensions were first determined from a powder pattern with Mo rays made by Mr. W. H. Dore of the Division of Plant Nutrition, University of California. This pattern showed no lines for which l is odd and hence led to a halved value of c. That the structure practically has a pseudo-cell with half the c dimension even resulted in the absence of odd layer lines on the first c axis rotation patterns. Finally these layer lines were detected on long exposure oscillation patterns and it was possible to observe a few lines with l odd on an excellent powder pattern with Co radiation.

The best determinations of cell dimensions were made from the two powder patterns mentioned after the indexing had been checked by other means.

It has long been customary among *x*-ray crystallographers to use the *x*-ray wave lengths based on Siegbahn's *assumed* grating space for calcite, 3.02904Å.[4] If this is done one should also use a value of Avogadro's number, or for the mass of atom of unit atomic weight which is consistent with these wave-lengths. Siegbahn[5] uses 60.594×10^{22} for Avogadro's number which he calls "Loschmidtsche Zahl." The reciprocal of this, 1.6503×10^{-24} grs., should be used as the mass of an atom of unit atomic weight together with the "Siegbahn" wave lengths. Unfortunately slightly different values have often been used.

Reconsideration of the general physical constants by various physicists has shown that the values used by Siegbahn have received notable correction by later work and that this largely reconciles the discrepancy which Siegbahn noted between his wave lengths and those obtained from line grating experiments. In a recent paper Donnay[6] used the value,

---

[4] See, for instance, *Handbook of Physics and Chemistry*, 23rd. ed. **1939**, *International Tables for the Determination of Crystal Structures*, vol. **II**, (1935), etc.

[5] Siegbahn, M., *Spektroskopie der Röntgenstrahlen*, p. 43 (**1931**).

[6] Donnay, J. D. H., Morphologie cristalline du groupe de la schéelite: *Trans. Roy. Soc. Canada*, **36**, 37–51 (1942).

60.23×10^{22}, for Avogadro's number, which he obtained from the results of Dunnington, to calculate the cell dimensions of members of the scheelite group from observed densities and goniometric constants. He compared the results of his calculations with cell dimensions for these minerals, determined in 1927 or earlier, with the use of Siegbahn wave lengths based on a different value of Avogadro's number. This procedure does not lead to comparable results.

TABLE 1. CELL DIMENSIONS AND DENSITY OF GILLESPITE

	Mass of atom of unit atomic weight	Unresolved K_α radiation		*a*	*c*	Density calc.
		λ_s	λ_b			
Berkeley Film Mo radiation cassette radius 203.2 mm.	1.6503×10^{-24} g.	0.7100	—	7.499	16.054	3.403
	1.66035×10^{-24} g.	—	0.7114	7.514	16.086	3.403
Cambridge Film Co radiation cassette radius 190.6 mm.	1.6503×10^{-24} g.	1.7872	—	7.491	16.046	3.412
	1.66035×10^{-24} g.	—	1.7908	7.506	16.078	3.412
Average values, Siegbahn system				7.495 ±0.010	16.050 ±0.010	3.407

The best consistent values of the physical constants presently available are doubtless those given by Birge.[7] In Table 1 are shown results of calculations for gillespite from two powder patterns. For each pattern the calculation is made in two ways, first using the customary Siegbahn wave lengths with the appropriate value of the mass of an atom of unit atomic weight, and then using the value for this constant given by Birge, together with wave lengths increased by the factor 1.002034, also given by Birge, to be consistent therewith. International Atomic Weights of 1939 were used. It may be noted that the ratio of the two values of the mass of an atom of unit atomic weight is just the cube of the ratio of the wave lengths and thus the calculated density is the same when consistent constants are used.

The calculated density is much higher than that reported by Schaller, 3.33, but agrees well with three determinations on clean fragments from California, 3.399, 3.404 and 3.402, average 3.402, with the Berman bal-

---

[7] Birge, R. T., A new table of values of the general physical constants: *Reviews of Modern Physics*, **13**, 233–239 (1941), and The general physical constants: *Reports of Progress in Physics*, **8**, 90–138 (1942).

ance. Two fragments from Alaska, furnished by Schaller, gave 3.390. All of my observed and calculated values lie within the range 3.40±0.02, corresponding to a cell content of 4 $BaFeSi_4O_{10}$. In view of the numerous checks it seems that both the Alaska and the California gillespite show no significant departure from Schaller's formula.

TABLE 2. SUMMARY OF OSCILLATION PATTERNS OF GILLESPITE, *c* AXIS, Co RAYS

hk ↓ *l*→	0	1	2	3	4	5	6
10			—		S		—
11	M*		S		VS		VS
20	VW		VS		VS		M
21		VW	M	—	—	—	W
22	S		M		M		M
30			W		VW		—
31	M	VVW	S	—	S	VW	S
32		VW	VW	—	M	—	—
40	VS		M		VW		S
41		W	—	—	W	VW	—
33	—		W		S		M
42	M	—	S	—	W	—	VW
50			—		M		—
43		W	W	—	—	VW	—
51	W	—	M	W	S	—	M
52		VW	M	—	—		VW
44	M		W		W		W
53	M	—	M	VW	M	—	M
60	M		S		M		VW
61		—	W	VW	—	—	—
62	M	—	M	—	M	—	W
54		W	VW	—	VW	VW	—
63		—	—	—	VW	—	—
70			W		—		—
71	M	—	M	W	M	—	S
55	W		M		—		—
64	S	—	M	—	W	—	M
72		VW	—	—	W		
73	VW	VW	S	W	S		
65		—	M				
80	M		M				
81		—	—				
74		W	W				
82	VS						

* From powder pattern.

Dashes indicate that "reflections" permitted in space group *P*4/*ncc* were not observed.

Vacant spaces correspond to the extinctions required by space group *P*4/*ncc*.

SPACE GROUP

Laue patterns indicate the Laue group 4/*mmm*. Table 2 shows a tabulation of all lines observed on *c* axis rotation and oscillation patterns. Appearance of $hk0$ with $h+k$ even only shows that 001 is an *n* plane and the appearance of hhl and $h0l$ with l even only shows that 110 and 100 are *c* planes. This indicates the space group $D_{4h}^{8}-P4/ncc$. Due to the *n* glide plane, odd layer lines of [110] rotation patterns are almost unoccupied and due to the *c* glide planes and absence of heavy atoms in general positions, the odd layers of [001] rotation patterns are very weak (Table 2).

DETERMINATION OF THE STRUCTURE

It is necessary to distribute 4 Ba, 4 Fe, 16 Si and 40 O among the positions:

4-fold	8-fold	16-fold
(*a*) $00\frac{1}{4}$ etc.	(*d*) $\frac{1}{4}\frac{1}{4}0$ etc.	(*g*) xyz etc.
(*b*) 000 etc.	(*e*) $00z$ etc.	
(*c*) $0\frac{1}{2}z$ etc.	(*f*) $xx\frac{1}{4}$ etc.	

A rough estimate of the x's and y's can easily be obtained from the observed intensities of the first few $hk0$ lines. It is unlikely that ions of such different radii as Fe and Ba should share a set of positions and the possibility of partially filled positions is set aside unless later considerations require that it be taken into account. With any distributions of Ba and Fe in the 4-fold positions these atoms give a maximum contribution to the 200 "reflection." Since this line is very weak, or absent, it follows that most of the lighter atoms must be clustered about a position with coordinates x, y somewhere near $\frac{1}{4}$, $\frac{1}{4}$. If these light atoms are so situated, 110 will be strong if both Fe and Ba are in positions (a) and (b), or if both are in positions (c), whereas the intensity of 110 would be weak to moderate if one of the heavy atoms is in (a) or (b) and the other in (c). Since 110 is observed as a weak line it seems that Ba is in (a) or (b) and Fe in (c), or vice versa, the choice between these possibilities being made after a more extended check of intensities.

From the fact that the ratio of Si to O is 2/5 and that gillespite has an excellent basal cleavage it seems certain that it has a silicate sheet structure. How such a structure may be reconciled with the requirements just outlined is shown in Fig. 1, in which SiO_4 tetrahedra are shown as triangles. In Fig. 1, *A*, *B* and *C*, each corner of an equilateral triangle corresponds to an oxygen atom and there is another oxygen atom above or below the center of each such triangle. Figure 1*A* shows the common hexagonal or pseudohexagonal Si_4O_{10} sheet found in micas and related minerals. It is also possible to make a tetragonal Si_4O_{10} sheet like that in

Fig. 1*B*. If the square groups of four SiO_4 tetrahedra are overlapped as in Fig. 1*C*, the tetrahedra in full lines pointing downward and those in broken lines pointing upward, form a continuous sheet of tetrahedra at

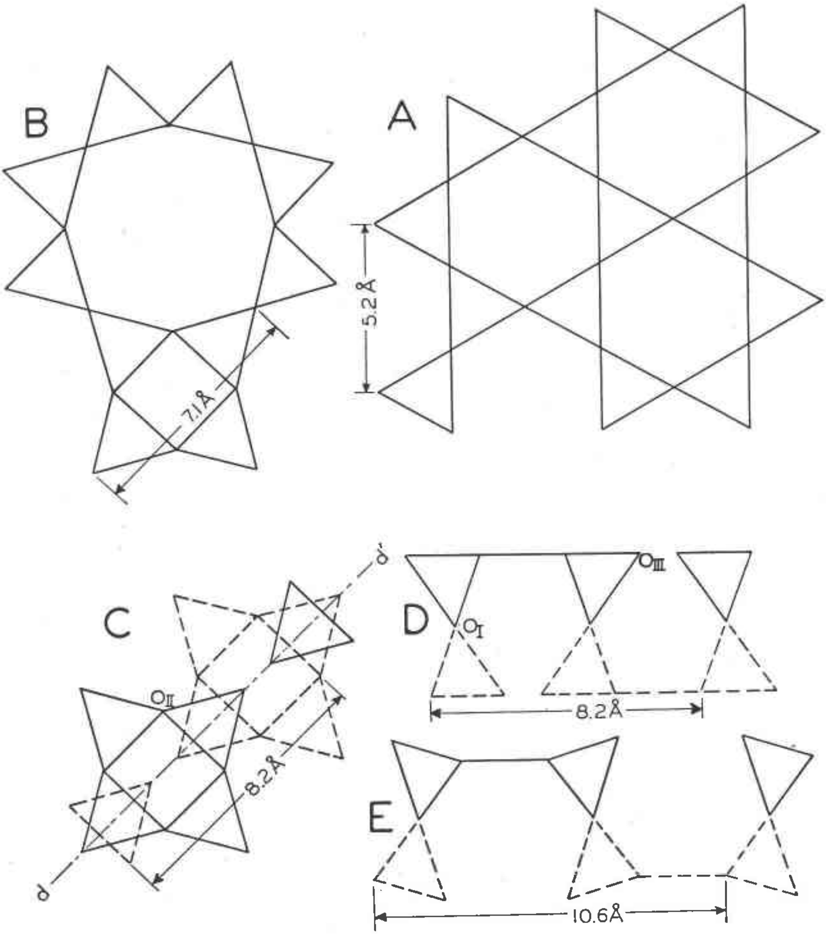

FIG. 1. Linking of SiO_4 tetrahedra to form Si_8O_{20} sheet.

two different levels, as shown in Fig. 1*D* which is a section through Fig. 1*C* along the line $d-d'$. In such a sheet the oxygens are of three different sorts, O_{III} at unshared corners, O_{II} (indicated in Fig. 1*C*) at corners shared by two tetrahedra at the same level, and O_I (indicated in Fig. 1*D*) at corners shared by two tetrahedra at different levels. There are, of course, an equal number of O_{III}'s and O_{II}'s and half as many O_I's.

The squares of Fig. 1*C* may be fitted about the 4-fold axes in position (*c*) leaving the overlapped tetrahedra clustered about $(x, y)=(\frac{1}{4}, \frac{1}{4})$.

The dimensions given in the several parts of Fig. 1 all depend on the assumption that the length of an SiO_4 tetrahedron edge is close to 2.6Å. The distance 5.2Å of Fig. 1*A* corresponds to the common *a* axis spacing of micaceous minerals. It will be seen that adjacent unshared corners, O_{III}, in Figs. 1*C* and 1*D* are much closer together than is compatible with the known oxygen radius. This can be corrected by canting the tetrahedra and expanding the sheet as shown in Fig. 1*E*. In this figure the operation has been carried just far enough so that the identity distance along $[1\bar{1}0]$ becomes 10.6Å, which is the value for gillespite.

The vertical dimension of such a sheet as that just described would be a little under 8Å and there would be 8 Si in a sheet within the cell limits. It follows that there are two sheets in a cell and O_I must be in position (*d*) $\frac{1}{4}\frac{1}{4}0$ or in (*f*) $xx\frac{1}{4}$, with x nearly equal to $\frac{1}{4}$, to correspond to the description just given. Assuming no deformation of tetrahedra it is possible to derive x and y coordinates for all atoms. Calculated intensities from such a structure give only a rough agreement of $hk0$ intensities, showing that a further shifting of the sheet is required. This is easily accomplished with 0_I in (*f*) $xx\frac{1}{4}$ by assigning to x some value other than $\frac{1}{4}$. The section shown in Fig. 1*E* then no longer lies in one plane but is offset as shown in the final picture of the structure, Fig. 4. Various values of x for O_I were tried in the range 0.20 to 0.25 with appropriate values of x and y for other atoms and the parameters given in Table 3 selected from intensity comparisons.

All intensity calculations were made with f values for Si^{+4}, O^{-2}, Fe and Ba taken from the International Tables for the Determination of Crystal Structures. Suitable plane frequency and glancing angle factors for rotation or powder patterns were used and no other corrections made.

Visual estimates of intensities were checked by photometer curves on the Co powder pattern and the zero layer lines of [uv0], [120], [110], [100] and [001] Co rotation patterns.

Table 3 shows that Ba must lie in position (*a*) or (*b*) whereas Fe is in position (*c*). The last column shows that there is no agreement of intensities if these two are interchanged. Patterns with Co radiation were chiefly used in all intensity comparisons to avoid the high absorption of Fe in gillespite for Cu radiation. In Table 3 a few observed and calculated intensities are also given for Cu radiation because they extend the range of agreement beyond the limit observable with Co rays and in this range of high glancing angles the effect of absorption is less serious. The only noteworthy discrepancies are the relative weakness of the observed intensities for 110 and 220 compared to calculated intensities. This is presumably due to absorption and/or extinction which may make itself felt for the first few lines even on patterns with Co rays and to the difficulty of accurate observation of intensities for rays scattered from the edges of a thin flake. A check is obtained by comparison of the

TABLE 3. OBSERVED AND CALCULATED INTENSITIES OF *hk*0 LINES OF GILLESPITE

Observed Intensities#					Calculated intensities x y x y Si 0.27 0.175 O_{II} 0.465 0.240 O_{I} 0.215 0.215 O_{III} 0.135 0.275		
Pattern	[010]	[110]	[001]		Ba in 0, 0 Fe in 0, 1/2		Ba in 0, 1/2 Fe in 0, 0
Radiation	Co	Co	Co	Cu	Co	Cu	Co
*hk*0							
110		1	1		22.2		59.6
200	—		—		5.4		5.4
220		5	5		120.0		120.0
310			4		37.8		10.6
400	4		10		91.5		91.5
330		—	—		1.3		16.6
420			4		62.8		
510			1		2.3		
440		2−	2		13.3		
530			3		15.5		
600	2−		3		15.8		
620			3		17.7		
710			3− }*		13.5		
550		—	1 }		2.4		
640			5		72.4		
730			—		4.4		
800	2−		4		43.8		
820			6	6	151.0	41.9	
660				—		4.9	
750				1		6.2	
840				2		31.0	

* These two lines are superposed in [001] rotation patterns. The observed intensities given for them are from oscillation patterns. All other observed intensities are from rotation patterns.

Scale of intensities; 1—very weak, 10—very strong.

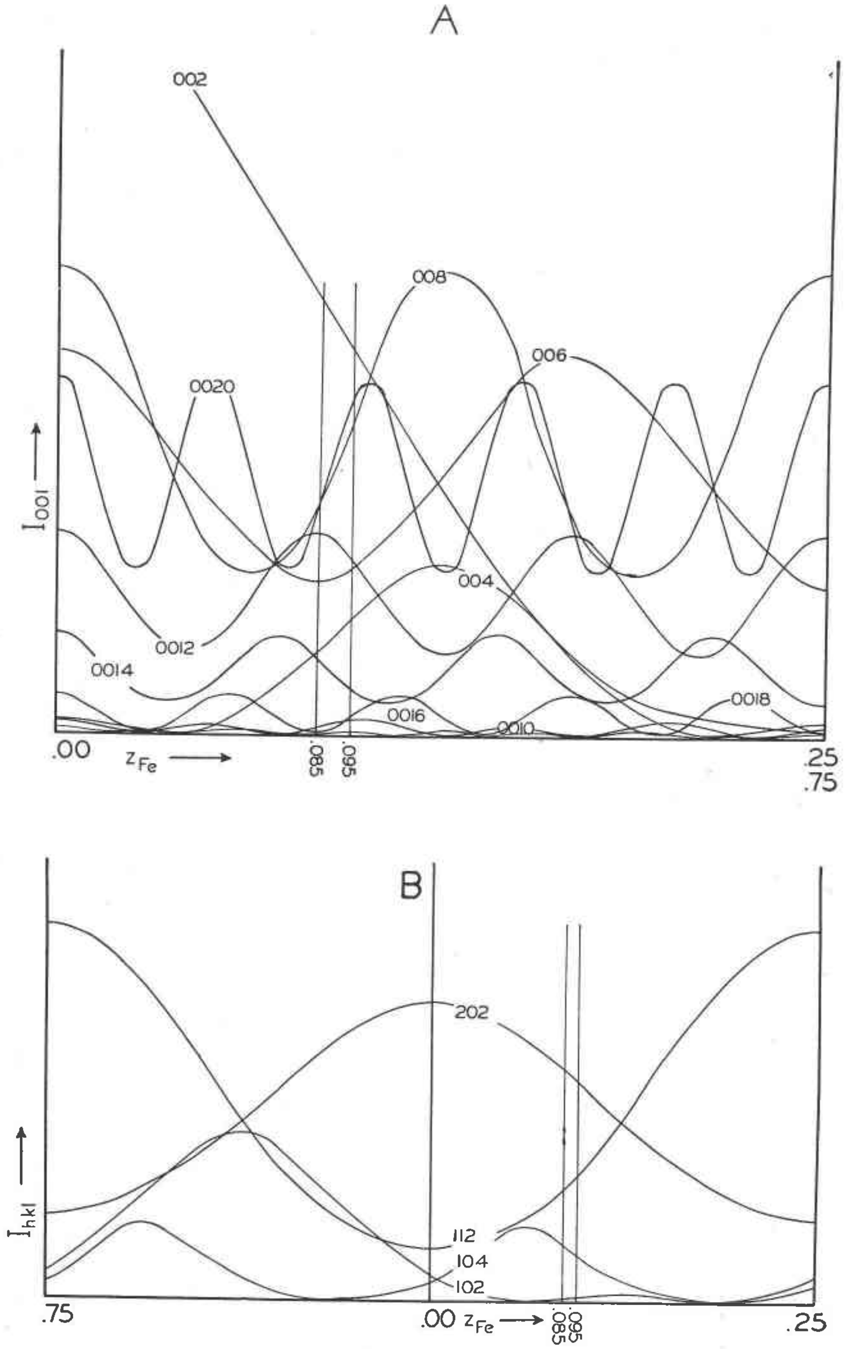

FIG. 2. *A*. Variation of 00*l* intensities with z_{Fe} when z parameters for other atoms are: Ba 0, Si .155, O_I $\frac{1}{4}$, O_{II} .14, O_{III} .095. Only even orders allowed by space group. Compare observed intensities (Cu) in Table 4.

B. Variation of intensities for a few pyramid planes with z_{Fe}. z for other atoms as in A. Compare observed intensities in text.

several orders of *h*00 and of *hh*0 on [010] and [1$\bar{1}$0] rotation patterns also shown in Table 3.

Accepting the values of *x* and *y* thus determined one can calculate the *z* for Si, O_{II} and O_{III} on the continued assumption that SiO_4 tetrahedra are essentially undistorted. This gives the following: $z_{Si}=.155$, $z_{O_{II}}=.14$ and $z_{O_{III}}=.095$.

It is now possible to select a parameter for Fe and to choose between positions (*a*) and (*b*) for Ba by consideration of intensities of 00*l*. A likely position for Fe would seem to be in 0, $\frac{1}{2}$, .095, where it would lie in a square of O_{III}'s at a distance of 1.97Å from each.

The observed intensity of 006<0012<008. From Fig. 2*A* it may be seen that a z_{Fe} parameter near the range .085 to .095 is in agreement with this. A discrepancy remains in the slightly low observed intensity of 002, which appears weaker than 008, but this may again be ascribed to absorption and/or extinction.

Figure 2*A* gives 00*l* intensities for Ba in (*b*) 000. If Ba is in (*a*) 00$\frac{1}{4}$, the calculated intensity of 0010 is high for any value of z_{Fe}. Since 0010 is not observed, this determines the choice of the position (*b*) 000 for Ba.

This still leaves z_{Fe} undetermined because all orders of 00*l* will show the same intensity with Fe in *z* or in $\bar{z}$, but in .905 or .915 Fe would be in quite a different position in the structure than in .095 or .085, remote from any O to which it may reasonably be expected to be tied. Fortunately it is easy to choose between these alternatives by considering only a few other lines. On a Co powder pattern the observed intensities of the first few lines due to pyramid planes are:—

102	112	104	202
absent	strong	medium	very strong.

Figure 2*B* shows clearly that the *z* parameter first selected for Fe yields excellent agreement and that the corresponding value $\bar{z}$ is not compatible with intensities.

It will be seen that in Fig. 2*A* the agreement of the intensities (compare Table 4) is slightly better when Fe is near .085 than when it is in .095, just within the square of O_{III}'s where one might expect it. The parameter .095 for O_{III} was calculated from the *x* and *y* parameters of the structure on the assumption that the SiO_4 tetrahedra are virtually undeformed. Actually small deformations have generally been found in well determined silicate structures. Nearly the same change in intensities of 00*l* as by shifting Fe from $z=.095$ to $z=.085$ can be obtained by shifting both Fe and O_{III} to $z=.09$. This results in only a trifling distortion of the SiO_4 tetrehedra and leaves the Fe just within the oxygen square. Intensity calculations for many lines were carried out for all three of these cases. Agreement is as good or better when Fe and O_{III} are both at $z=.09$ and so this was chosen for the final set of parameters:

		x	y	z			x	y	z
4	Ba (b)	0	0	0	8	O_I (f)	.215	.215	$\frac{1}{4}$
4	Fe (c)	0	$\frac{1}{2}$	.09	16	O_{II} (g)	.465	.24	.14
16	Si (g)	.27	.175	.155	16	O_{III} (g)	.135	.275	.09

Tables 4 and 5 show the calculated intensities corresponding to these parameters and the observed intensities on various films. Agreement is satisfactory throughout.

Table 4. Observed and Calculated Intensities of Spots on Some Rotation Patterns of Gillespite

$00l$						$h0l$		
Observed				Calculated		Observed		Calculated
Rotation axis	[uv0]	[110]	[120]				[010]	
Radiation	Cu	Co	Co	Cu	Co		Co	Co
002	5	6	5	68.2	60.5	102	—	1.8
004	4	5	5	10.7	9.1	104	5	43.5
006	6	7	7	19.3	15.9	202	6	155.0
008	10	10	10	30.6	24.6	204	5	60.4
0010	—	—	—	0.9	0.7	106	—	1.0
0112	8	8	8	26.5	24.4	302	1	7.6
0014	5	4	5	10.5	11.2	206	1—	5.6
0016	—	—	—	0.3	0.5	304	—	1.5
0018	—			0.3		108	4	18.3
0020	6			32.9		306	2#	0.6#
						402		14.6#
						208	1	9.6
						404	—	2.7

Coincidence, compare table 2, where 306 is absent and 402 medium.

FOURIER ANALYSES

The structure of gillespite may be conveniently checked by fourier analyses. A one-dimensional summation can be made which gives the electron density projected upon the c axis,

$$\rho_z \sim \sum_{0}^{l} F_{00l} \cos 2\pi lz.$$

TABLE 5. OBSERVED AND CALCULATED INTENSITIES FOR A PATTERN OF GILLESPITE WITH CO RADIATION

hkl	Height of photometer curve peak	Calculated intensity	*hkl*	Height of photometer curve peak	Calculated intensity
002	6.0 mm.	1,086	322	2.5 mm.	145 { 34
102	—	45	008		111
110	2.5	263	323	2.0	168 { 13
112	8.5	1,334	108		155
004	2.5	117	315	—	21
200	—	41	217	—	2
104	4.5	678	226	—	61
202	14.0	2,329	118	5.0	580 { 196
211	4.0	200	400		384
114	11.5	1,466	324	1.0	172
212	4.5	385	306	0.5	124 { 5
213	—	9	402		119
204	6.5	713	411	—	60
006	6.0	822 { 93	316	4.5	620 { 614
220		729	412		6
214	0.5	63	208	—	77
106	2.5	365 { 12	330	—	5
222		353	325	—	6
116	8.0	987 { 700	332	0.5	83 { 82
302		82	413		1
310		205	218		0
311	—	27	404	—	21
215	—	0	420	1.0	236
312	3.5	452	421	—	1
224	2.5	259	414	—	68
206	1.5	58 { 54	317	—	0
313		4	326	2.5	424 { 1
304	—	15	422		423
216	1.0	54	334	1.5	265
321	1.0	65	0010	—	2
314	4.5	482			

The F values were taken to be

$$\sqrt[2]{\frac{I_{\text{obs}}}{\dfrac{1+\cos^2\theta}{\sin 2\theta}}}$$

without further correction. Only one quarter of the cell height need be calculated since the projection of the structure onto the *c* axis is symmetrical at 0, $\frac{1}{4}$, $\frac{1}{2}$, etc. The Lipson and Beevers strips can be used to great advantage in this case. If the l's of all observed $00l$'s are halved (only even l allowed by space group) and results plotted for a pseudocell of $c/2$, points are obtained at each 1/120 of the true cell height instead of the usual 1/60 when these strips are used. By calculating a few additional points near $z=.09$ and $z=.15$ a very satisfactory projection of the electron density onto the c axis, almost a side view of the structure, is quickly obtainable. The result is shown on the left side of Fig. 3. The peaks corresponding to Ba, Fe and 4 O_{III}, 4 O_{II} and 4 Si, and to 4 O_I appear at the levels of the z parameters previously chosen. These peaks also are of such sizes as correspond closely to the numbers of scattering electrons situated at the several levels.

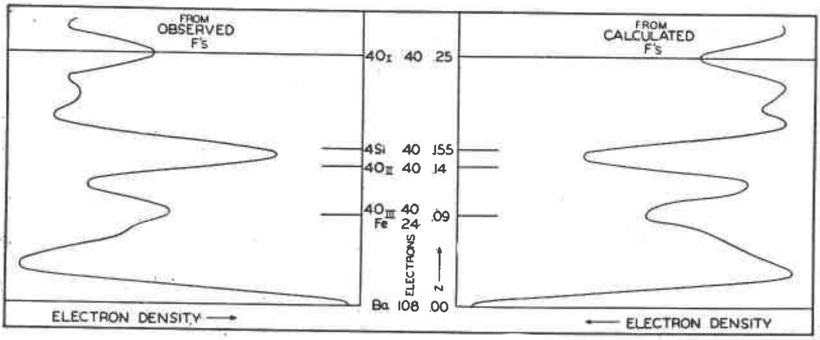

FIG. 3. Electron density as a function of z for one quarter of the cell height of gillespite from fourier summations of observed and of calculated F's.

There is a small peak near $z=.21$. It can be seen that this is spurious and not due to any other scattering matter at this level by comparing with the ideal curve shown on the right of Fig. 3 which shows a similar peak near this level. This is due simply to the limited number of orders available for the summation.

Since the basal projection of the gillespite structure has a center of symmetry it is feasible to make a fourier summation for it from observed intensities of $hk0$ lines. For this it is necessary to make summations over only 1/16 of the area, but it was found convenient, again using the Lipson and Beevers method, to make summations for $\frac{1}{8}$ of the area, $\frac{1}{2}a\times\frac{1}{4}a$, affording a complete check of the result.

The contoured fourier diagram is shown in the upper left quadrant of Fig. 4. The details of the silicate sheet are somewhat obscured by the superposition of many atoms in the projection, as shown in the upper right quadrant.

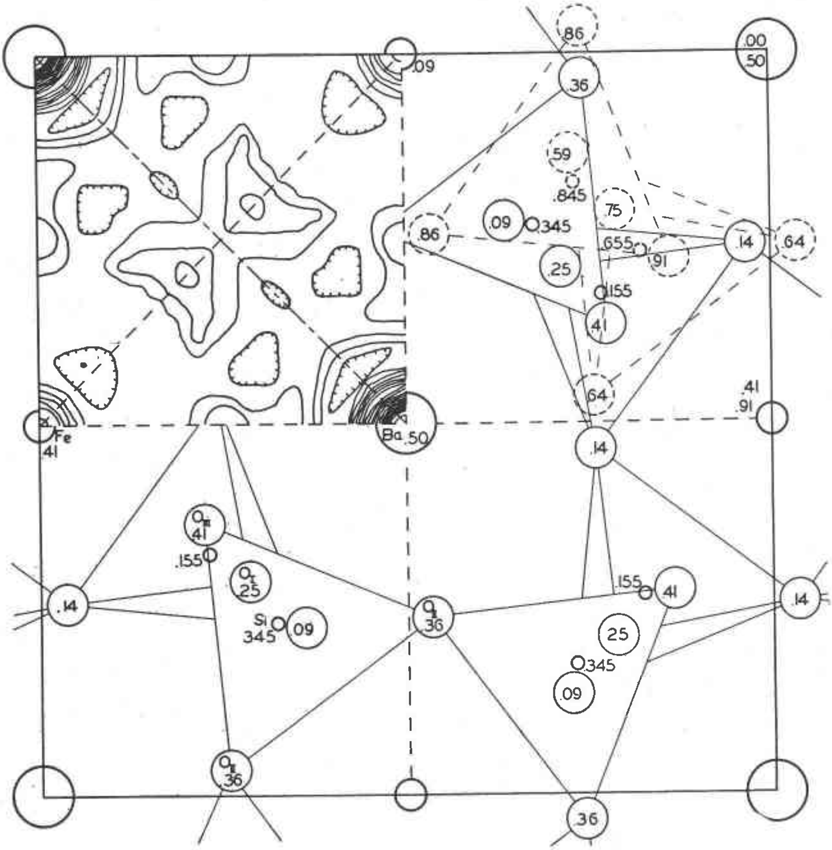

FIG. 4. Structure of gillespite projected onto 001. Lower half of diagram shows only one Si_8O_{20} sheet. In the upper right the other sheet is shown by broken lines. Upper left is electron density diagram obtained by fourier summation.

DISCUSSION OF THE STRUCTURE

In the lower part of Fig. 4 only one of the silicate sheets in the cell is shown in order to bring out the linkage. In the lower left quadrant the labelled Si is at the center of the tetrahedron with labelled O's at the corners. The labelled Fe and Ba are those closest the O_{III} corner of this tetrahedron. Other atoms are identified merely by their z coordinates and circles of appropriate sizes.

The entire upper Si_8O_{20} sheet is derivable from the lower sheet by glide reflection on the n plane in $xy0$ or $xy\frac{1}{2}$. This operation can be seen in the diagram by the glide reflection of the tetrahedra shown in full lines in the lower left to the positions shown in dashed lines in the upper right quadrant.

Both Ba and Fe lie between the sheets, but each Fe is at a minimum distance or bound to the O_{III}'s of only one sheet, whereas Ba is at a minimum distance or bound to O_{III}'s in both the upper and lower sheets, as the following tabulation shows:

	x	y	z	
Labelled Fe in Fig. 4	$\frac{1}{2}$	0	.41	
	.635	.225	.41	
nearest	.275	.135	.41	lower
O_{III}'s	.365	.775	.41	Si_8O_{20} sheet
	.725	.865	.41	
Labelled Ba in Fig. 4	$\frac{1}{2}$	$\frac{1}{2}$	$\frac{1}{2}$	
	.635	.225	.41	lower
nearest	.365	.135	.41	Si_8O_{20} sheet
O_{III}'s	.775	.635	.59	upper
	.225	.365	.59	Si_8O_{20} sheet.

Each Si_8O_{20} sheet has four oxygens (O_{III}) bound to but one silicon on its upper side and four on its lower side within each cell. Each such oxygen is tied to one Ba and one Fe. Since all of the O_{III}'s tied to each Fe are in the same sheet it follows that each Fe belongs definitely to a particular sheet, whereas each Ba is tied to O's above and below. In this way successive sheets are held together by the larger positive ions and the smaller positive ions lie within a single sheet. To this extent the linkage of this structure resembles that of micas.

TABLE 6. INTERATOMIC DISTANCES IN GILLESPITE

Edges of SiO_4 tetrahedron		Si –O_I	1.59Å
O_I –O_{III}	2.67Å	Si –O_{II}	1.56
O_I –O_{II}	2.58		1.59
	2.59	Si –O_{III}	1.64
O_{II} –O_{II}	2.63	Fe–O_{III}	1.97
O_{III}–O_{II}	2.59	Ba–O_{III}	2.73
	2.63	Ba–O_{II}	2.98

The interatomic distances in Table 6 show excellent agreement with expected values. Ba is found to have eight-fold coordination.

The four-fold coordination of Fe is unusual for this element, but since the four oxygens are arranged in a square which is centered on the iron this is like octahedral coordination with a pair of opposite octahedron corners unoccupied. Such a coordination has not previously been reported for iron in silicates, but is known for several elements in other types of compounds. The arrangement of four (CN) groups in a square about Ni has recently been found in $BaNi(CN)_4 \cdot 4H_2O$.[8]

RELATED STRUCTURES

The mineral most closely related to gillespite in composition is the triclinic sanbornite, $Ba_2Si_4O_{10}$, with which it is found in California.[9] Professor Rogers cautiously stated "It seems likely that sanbornite has a structure similar to that of micas and related minerals, though there is no direct evidence that it is pseudohexagonal." He then described a pseudohexagonal structure which he pictured as "probable." It may well be that sanbornite is pseudohexagonal even though closely similar to gillespite in composition. It has been shown that the roles of Fe and Ba in the gillespite structure are very different. Substitution of Ba for Fe to give the composition of sanbornite might be expected to result in a different linkage of the Si_4O_{10} sheets and possibly a different structure of the sheets themselves. A powder pattern of a triclinic mineral cannot be very illuminating, but at any rate, such a pattern made from sanbornite showed no similarity with powder patterns of gillespite.

So far as the writer is aware only one of the classifiers of silicate structures has included gillespite and sanbornite in his considerations. They were classed as "*anhydrous non-aluminum disilicates*" by Berman[10] without benefit of x-ray evidence.

In the enumeration of possible silicate structures it is usually stated or implied that "tetrahedra combined by three solid angles" produce sheets of indefinite extent.[11] Though all known structures with three shared tetrahedron corners throughout are sheet structures there are other geometrical possibilities. One might have double rings of tetrahedra. If, for instance, two trigonal Si_3O_9 rings, such as occur in benitoite, were placed one upon the other and tetrahedron corners shared between

---

[8] Brasseur, H., and de Rassenfosse, A., Structure cristalline des cyanures doubles de baryum a base de platine, de palladium et de nickel: *Bull. soc. fran. min.*, **61**, 129–136 (1938).

[9] Rogers, *op. cit.*

[10] Berman, H., Constitution and classification of the natural silicates: *Am. Mineral.*, **22**, (Palache number) 342–408 (1937).

[11] Schwartz, C. K., Classification of the natural silicates: *Am. Mineral.*, **22**, 1075 (1937).

them, a double ring, Si_6O_{15}, would result. Double rings of like Si/O ratio with three corners of each tetrahedron shared might also be tetragonal, hexagonal or pseudohexagonal. Such structures would not conflict with known requirements of ionic radii or tetrahedron linkage.

In some respects the structure of gillespite resembles that of apophyllite,[12] the formula of which is best written $KF \cdot Ca_4Si_8O_{20} \cdot 8H_2O$. There are two such units[13] in the cell of dimensions $a = 9.00$Å, $c = 15.8$Å and the space group is $D_{4h}^6 - P4/mnc$. The linkage of tetrahedra is similar to that of gillespite, there being two Si_8O_{20} sheets parallel to the base in each cell, with unshared tetrahedron corners pointing alternately upward and downward on either side of each sheet. The bonding of sheet to sheet, however, is quite different, involving also F and OH in the coordination about the positive ions.

LEACHING OF GILLESPITE

Schaller[14] reported that gillespite can be leached with the complete removal of iron and barium. The glistening flakes which remain are uniaxial negative like gillespite, but the mean index drops to about 1.45. The flakes take up a great deal of water and Schaller considered them, on the basis of quantitative determinations, to have changed in composition from $8SiO_2 \cdot 2FeO \cdot 2BaO$ to $8SiO_2 \cdot 2H_2O \cdot 2H_2O \cdot H_2O$. Assuming that the new material occupies exactly the same volume as the original its density would be expected to be 2.08. Any lower density would be indicative of loosening of the structure attending leaching or of swelling upon hydration.

The leaching experiments were repeated, confirming all of Schaller's observations, and the density of the colorless leached flakes was found to vary between 1.8 and 2.0, mostly near 1.9, showing that little, if any, swelling occurs. Under the circumstances one might expect to find the silicate sheet structure retained in the leached, hydrated material. Attempts to observe *x*-ray diffraction in the leached material by powder and rotation methods led to negative results, but a long exposure Laue pattern, made with the aid of an intensifying screen, with beam normal to the base of a well leached flake still shows a very faint tetragonal design (Fig. 5) on which half a dozen spots may be roughly measured in each quadrant. By contrast, over a hundred spots are measureable in

---

[12] Taylor, W. H., and St. Náray-Szabó, The structure of apophyllite: *Zeits. Krist.*, **77,** 146–158 (1931).

[13] Not four, as stated by Bragg in *Atomic Structure of Minerals*, p. 227 (1937).

[14] Schaller, W. T., The properties and associated minerals of gillespite: *Am. Mineral.*, **14,** 319–322 (1929).

one quadrant of a similar pattern made from fresh gillespit. At most only a faint trace of the structure of gillespite is retained in the leached flakes.

The leaching or "bleaching" of biotite by acid solutions, a process that also occurs widely in nature, has long been familiar to mineralogists. A recent study[15] of the leaching of biotite has again shown that the fully leached material is amorphous to *x*-rays when examined by the powder method, as long ago reported by Rinne. While the flakes remain uniaxial negative their mean index drops as low as 1.43.

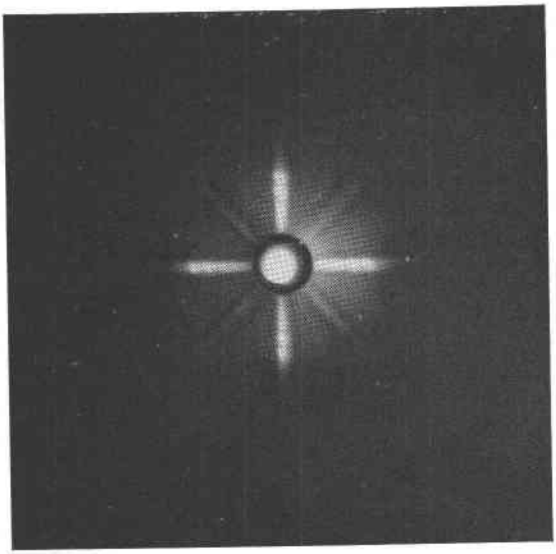

FIG. 5. Laue pattern of leached gillespite. Beam normal to 001.

The writer has leached dark biotite from the Half dome quartz monzonite west of Tenaya Lake in Yosemite National Park[16] with an initial density of 3.03 and mean index of about 1.65. The final leaching product gives no powder diffraction pattern, has a density of 1.7 – 1.8 and a water content (ignition loss) of nearly 11%.

Bailey[17] has recently described apophyllite from California naturally

[15] Mehmel, M., Ab- und Umbau am Biotit: *Chemie der Erde*, **11**, 307–332 (1937).

[16] This is doubtless the same or nearly the same as the biotite analyzed by Hillebrand and reported by H. W. Turner, Some rock-making biotites and amphiboles: *Am. Jour. Sci.*, (4) **7**, 294–298 (1899), from "Tioga road southeast of Mt. Hoffmann."

[17] Bailey, E. H., Skeletonized apophyllite from Crestmore and Riverside, California: *Am. Mineral.*, **26**, 565–567 (1941).

altered to a material which is largely hydrated silica and retains the uniaxial negative character of fresh apophyllite though its mean index is only 1.44. Others have previously described similar occurrences. Bailey supposes the apophyllite to have "undergone a selective leaching process" "without destroying the framework of the crystals." He also failed to observed *x*-ray diffraction by the powder method in the leached material.

It seems that changes produced by leaching in apophyllite, gillespite, and biotite with removal of cations and addition of water are very similar. The flakes retain their shape and some of their optical properties but yield no *x*-ray diffraction pattern when examined by the powder method.